

Construct and Performance Investigation of a Hybrid ANFIS Controlled Islanded Micro-Grid

A. Venkat Rao [†] , G. Suresh Babu ^{**} , P. Satish Kumar ^{*} , Pothula Jagadeesh ^{***} ,
M. Mallikarjuna Reddy ^{****} , B.V. Sai Thrinath ^{*****} , Ramprasad Vangalapudi ^{*****} ,
N. Vasantha Gowri ^{*****} 

^{*} Department of Electrical Engineering, Osmania University, Hyderabad, Telangana, India

^{**} Department of Electrical and Electronics Engineering, Chaitanya Bharathi Institute of Technology, Telangana, India.

^{***} Department of Electrical and Electronics Engineering, Sagi Rama Krishnam Raju Engineering College, Bhimavaram, Andhra Pradesh, India.

^{****} Department of Electrical and Electronics Engineering, Sir C R Reddy College of Engineering, Eluru, Andhra Pradesh, India.

^{*****} Department of Electrical and Electronics Engineering, Mohan Babu University, Tirupathi, India

^{*****} Department of Mechanical Engineering, Sreenidhi Institute of Science and Technology, Hyderabad, India,

^{*****} Department of Electrical and Electronics Engineering, Chaitanya Bharathi Institute of Technology, Telangana, India, 500075

(venki.aarepalli@gmail.com, gsureshababu_eee@cbit.ac.in, satish_8020@yagho.co.in, jagadeesh.pothula@gmail.com, mallikarjuna.madire@gmail.com, connectbvst@gmail.com, ramprasadgurukul@gmail.com, vasanthagowri_eee@cbit.ac.in)

[†]

Corresponding Author: A. Venkat Rao, Osmania University, Hyderabad, Telangana, India, Tel: +91-8885851666, venki.aarepalli@gmail.com.

Received: 04.08.2023 Accepted:01.10.2023

Abstract: This study presents an innovative approach to enhance the performance of a microgrid utilizing solar photovoltaic, wind, and battery energy storage. This system incorporates an intelligent adaptive neuro-fuzzy interface, operating in conjunction with a shunt voltage source converter. Notably, the design incorporates a self-tuning filter, eliminating the need for phased locked loops, as well as low and high pass filters. Furthermore, the self-tuning filter serves the dual purpose of achieving phase synchronization while effectively isolating harmonic and fundamental components. To control this system, a hybrid ANFIS controller is employed. The primary goal of this proposed method is twofold: firstly, to reduce THD, and secondly, to maintain a stable voltage across the DC link capacitor, with rapid settling times under both grid-connected and islanded conditions. To assess the system's performance, a comprehensive analysis is conducted across four distinct scenarios, encompassing various combinations of loads, solar irradiation levels, and wind velocities during islanding conditions. Additionally, a comparative evaluation is carried out against conventional methods such as PIC, SMC, and ANNC and also methods in state of art of literature.

Keywords- Self tune shunt active power filter, total harmonic distortion, solar PV system, wind system, battery energy storage.

Nomenclature:

R_s, L_s	Grid Resistance and Inductance	V_{se_abc}	Series filter supplied voltage in abc phases
$i'_{l_\alpha\beta}, i'_{l_d\beta}$, and i'_{l_dq}	FC and HC of load current in $\alpha - \beta - 0$ and dq domain	$V^{ref}_{abc}, V^{ref}_{dq}, V^{ref}_{\alpha\beta}$	Reference voltages for phases abc, dq and $\alpha - \beta - 0$ domain

$V_{se_dq}^{ref}$, and	compensated reference's voltage in $d - q$ and $\alpha - \beta - 0$	CE	Change in error
$V_{se_\alpha\beta}^{ref}$		LPF/ HPF	Low and high pass filters
V_{l_abc}	Voltage across the load in abc phases	PLL	Phasor locked loop
$i_{l_abc}^{ref}$, $i_{l_\alpha\beta}^{ref}$, $i_{l_dq}^{ref}$	Reference load current in abc, $\alpha - \beta - 0$ and dq	PIC	Proportional integral controller
C_{sh}	Capacitance of shunt filter	UVG	Unit vector generation
$V_{S_ \alpha\beta}$	Source voltage in $\alpha - \beta - 0$ domain	FC	Fundamental component
R_{sh}	STAPF Resistance	HC	Harmonic component
P_{PV}	Output power of solar PV	DLCV	Dc link capacitor voltage
$i_{S_ abc}$	Source current for abc phases	STAPF	Self tuning active power filter
L_{sh}	STAPF Inductance	SRFT	Synchronous reference frame theory
C_{dc}	Capacitance of the capacitor across DC-Link	FF-ANNC	Firefly based artificial neural network controller
V_{dc}	DLCV	PV	Photo voltaic
$i_{sh_ abc}^{ref}$	Reference shunt filter supplied current in abc	DSTATCOM	Distributed static compensator
V_{dc}^{ref}	Reference DLCV	GW-O	Grey wolf optimization
$V'_{S_ \alpha\beta}$	FC of grid voltage in $\alpha - \beta - 0$ domain	PQ	Power quality
$P_{DC-Link}$	Power at DC link	ANN	Artificial neural network
$V_{S_ abc}$	Supply voltage in abc phases	ANFIS	Artificial neuro fuzzy controller
P_{BSS}	Battery Power	AC-O	Ant colony optimization
$i_{sh_ abc}$	Series filter supplied current in abc	ANNC	Fuzzy logic based proportional integral controller
E	Error	B-C	Boost converter
Δi_{dc}	DC link error	B-B-C	Buck boost converter
$i_{l_ abc}$, $i_{l_ \alpha\beta}$	Load current in abc and $\alpha - \beta - 0$	SPG	Solar power generation
SMC	Sliding mode controller	SOCB	State of charge of battery
UPQC	Unified power quality conditioner	$SOCB_{min}$	Lower limit of SOCB
FACTS	Flexible ac transmission system	$SOCB_{max}$	Upper limit of SOCB
FL-C	Fuzzy logic controller	MF	Membership function
		PWM	Pulse width modulation
		SRAPF	Series active power filter
		BES	Battery storage system
		PS-O	Particle swarm optimization
		MF	Membership Functions
		STF	Self tuning filter
		VSC	Voltage source converter
		SPS	Solar power system

1. Introduction

Due to the association of renewable sources and usage of power electronic devices leads to the generation of PQ problems in the distribution network. The handling of the adverse effects of these issues becomes a challenge to the power engineers. Along with the recent advancements, the various control techniques and configurations of SAPF was discussed for three phase distribution network [1]. The SRFT controller was suggested for the four 3phase distribution network during the balanced and unbalanced loads [2].

1.1. Literature Review

A FL-C and PI-C properties was combined to develop a hybrid controller for STAPF with an intention of diminishing the THD for different types of loads [3]. Besides, the STF based STAPF was developed for managing reactive /real powers along with the current signal THD [4]. Further, advancement in the artificial intelligence control methods like FL-C, ANNC etc for STAPF addresses PQ issues successfully during the dynamic power system load variations [5-7]. The PV system with MPPT was suggested for UPQC and its performance was analyzed under variable loading conditions with a view of minimizing THD [8]. Besides, PI-C was suggested for SRFT based control signal generation for the STAPF connected to fuelcell with an aim of enhancing the current waveform shape and stabilizing DLCV [9]. The hybrid control technique with both characteristics of FLC and ANN was recommended for UPQC to minimize the grid voltage and current waveforms imperfections with DLCV balancing for dynamic loads [10]. On other hand, to regulate the DLCV and to handle reactive power FF-ANNC was designed for PV/wind associated UPQC [11].

The firefly optimization was used to train ANNC was developed for the shunt VSC for the PV/battery UPQC to reduce the MSE and minimize THD [12]. Besides, the DVR/DSTATCM was integrated to the solar, wind and fuel cell micro-grid to address the current and voltage related PQ issues [13]. However, the UPQC was suggested to handle the PQ problems generated due to the nonlinear electric arc furnace load. Furthermore, a comparison was made with the performance of DSTATCOM [14]. The intelligent controller in the association of both ANN and FL-C properties was implemented for PV integrated UPQC to handle PQ troubles under load variations [15]. The STAPF with STF was developed to avoid the requirement of LPF's and PLL to diminish the THD. On other hand, the results are validated with experimental setup [16].The FL-C was developed for UPQC for different non-linear loads to suppress the distortions in current and thereby enhancing the THD [17]. Besides, the Fourier analysis was advised for renewable sources, solar in combination with wind and fuel cell with a view of diminishing the THD [18].

The meta-heuristic BBO algorithm was chosen for the optimal selection of PI-C gain parameters along with DLCV balancing and also to improve the fast response in fault condition [19]. A new metaheuristic HBO was proposed from the intelligent hunting behavior of honey badgers with a motive for solving optimization problems. Besides, the fuzzy-based hybrid technique was adopted to achieve maximum out

of PV. However, to reduce the complexity the ANN was considered for UPQC reference signal generation to sole PQ issues [20]. Besides, the fuzzy back propagation method was suggested for the 5level UPQC to handle PQ issues [21]. The soccer optimization was chosen for the best design of an ANN controller to reduce THD in a local distribution network [22]. A novel game based soccer league algorithm was selected for PI-C for the selection of gain parameters along with the filter parameters to address both voltage and current related PQ problems [23].

It was investigated [24] the advantages and difficulties of integrating renewable energy sources into the system and their control strategies. A few recommendations were also made to transform the conventional grid into a smart grid, and the implications of smart grid technologies on the national grid were underlined [25]. For changes in solar irradiation, the comparison of P & O and PSO algorithms to provide MPP for the PV system was investigated [26]. Integration of renewable sources to micro grid for MPPT was studies with power management [27]. High voltage isolated ACDC converters were developed based on the modular technology [28]. Fuzzy logic controller was suggested for PV-MPPT to improve the overall performance by maximum power point tracking [29].

1.2. Contribution and Paper Alignment

In this paper, ANFIS is suggested for the micro-grid is associated to STAPF with an intension of stabilizing DLCV during load variations with lowest settling time, along with reduction in THD as an objective function under islanding condition. The STAF is proposed to avoid the necessity of PLL, LPF and HPF. To demonstrate the effectiveness of ANFIS four various test studies is carried out, and to show the viability of the suggested method comparison was done with PI-C, SM-C and ANNC. The paper is aligned into Section 2 gives the proposed system description, Section 3 provides the control strategy, Section 4 and Section 5 give the control method, simulation results with discussion, and finally Section 6 ends with Conclusion.

2. System Description

The developed STAPF with components are illustrated in Fig. 1. A DC Link connects the microgrid to the STAPF through B-C for solar PV and B-B-C for battery. The prime role of shunt connected VSC is to diminish the current THD through supplying required compensating current in addition to DLCV balancing. The micro-grid with solar, wind and battery energy systems are external fed to the STAPF in order to regulate the DLCV balancing under variable loading conditions. However, the main advantage of external renewable source support reduces the required ratings and stress of the converters. Table. 1 provides the micro-grid parameters chosen in this paper. The dispersion of power for proposed STAPF at the capacitor is exhibited by Eq. (1) and explanation is given in Table 2.

2.1. Solar PV System

The solar PV system transfers solar irradiation into electricity, depends on the number of PV modules connected in series and parallel. The solar PV system transfers solar

irradiation into electricity, depends on the number of PV modules connected in series and parallel. In the module, every PV cell is modeled by using single diode equivalent circuit as displayed in Fig 2.

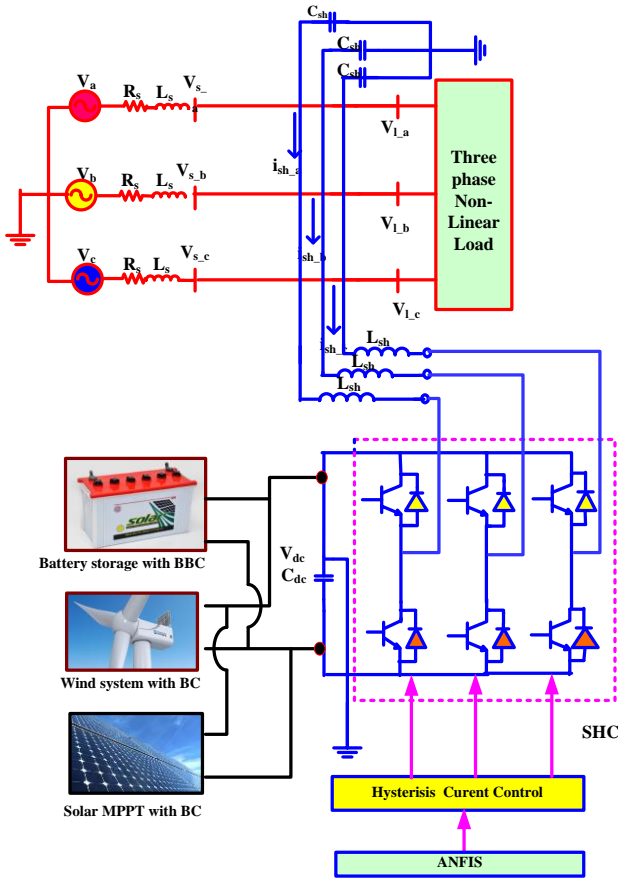


Fig.1. Components of STAPF.

$$P_{PV} + P_{BS} - P_{DC} = 0 \quad (1)$$

It consists of photo current source (i_{ph}) with forward diode carrying current (i_d), a series and parallel cell resistances ($R_{s,PV}$ and $R_{sh,PV}$) carrying current of (i_{PV} , $i_{sh,PV}$). The PV cell identifies sun irradiation and converts it into current. By adopting KCL, PV cell output current (i_{PV}) is obtained by Eq. (2)

$$i_{PV} = i_{ph} - i_d - i_{sh,PV} \quad (2)$$

Where,

$$i_d = i_{rev,sat} \left(e^{\frac{V_d}{\eta V_T}} - 1 \right)$$

$$i_{rev,sat} = K(T^m) \left(e^{\frac{-V_{G0}}{\eta V_T}} \right) \text{ and} \quad (3)$$

$$V_T = \frac{K_B}{q} T$$

Here, $i_{rev,sat}$ is the reverse saturation current, K constant value varies by material properties, V_{G0} is the band gap of material considered in eV, q is the charge, K_B is the Boltzmann constant, T is temperature, η is diode identity factor. By,

substituting Eq. (3) in Eq. (2), we obtain current of cell by Eq. (4)

$$i_{PV} = i_{ph} - i_{rev,sat} \left(e^{\frac{V_d}{\eta V_T}} - 1 \right) - \frac{V_{PV} + I_{PV} R_{sh,PV}}{R_{sh}} \quad (4)$$

Where, G , G_n represents solar irradiance (W/m^2) and at STC, ΔT_C variation in temperature. To enhance the output of PV the Incremental conductance algorithm based MPPT was adopted in this work. The output of solar system (P_{PV}) is calculated by Eq. (5). The PV cell characteristics at various irradiation and constant temperature 25^0c are given in Fig. 3. The control system is given in Fig. 2

$$P_{PV} = V_{PV} \cdot I_{PV} \quad (5)$$

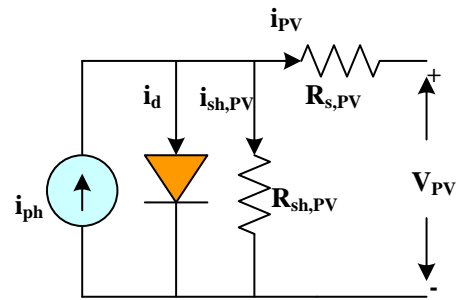


Fig. 2. PV cell model.

Table 1. PV, wind, BSS ratings.

Equipment	Factor	Value chosen
PV single panel (Sun power SPR-215-WHT-U)	PV cells connected in parallel, series	66, 5
	Rated Power	305.226W
	Short circuit current	5.98A
	Open circuit voltage	64.2V
	Under max power the voltage & current	54.7V /5.58A
	Fully charge voltage	350V
Li-ion battery	Rated Capacity	350Ah
	Cut off voltage	262.5V
	Normal Voltage	405V
Wind Turbine	Nominal turbine mechanical power	4 MW
	Base power of the electrical generator	400e3/0.9
	Base wind speed	11 m/sec

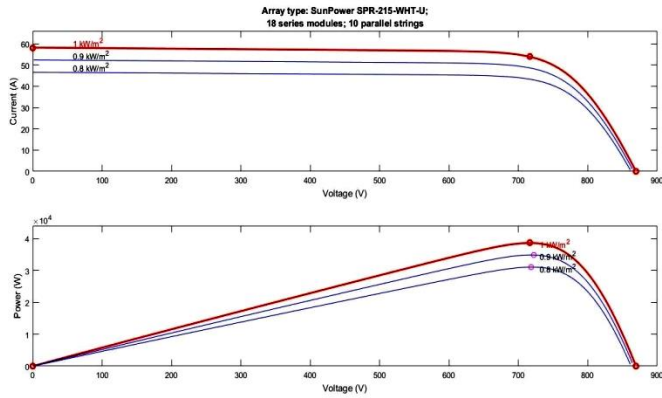


Fig. 3. PV cell characteristics at various irradiation and constant temperature 25°C.

To enhance the output of PV the Incremental conductance algorithm based MPPT was adopted in this work. The output of solar system (P_{PV}) is calculated by Eq. (6). The control system is given in Fig. 4

2.2. Battery System

Battery’s charging and discharging mode of operation is based on the amount of SPG while satisfying the constraints of $SOCB$ to maintain DLCV. $SOCB$ is evaluated by Eq. (6) and its limits are given in Eq. (7). The modes of operation at DC link are given in Table 2. The control system is given in Fig. 4

$$SOCB = 70(1 + \int i_{BS} dtQ) \quad (6)$$

$$SOCB_{min} \leq SOCB \leq SOCB_{max} \quad (7)$$

2.3. Wind System

The wind generated AC voltage is rectified into DC voltage, which is then boosted through a boost converter. Permanent magnet synchronous machine was considered in the present work. The wind power generation as shown in Fig. 4 is given by Eqs. (8) - (12).

$$P_m = 1/2\pi \rho C_p(\lambda, \beta) R^2 V^3 \quad (8)$$

$$\lambda = \frac{\omega_m R}{v} \quad (9)$$

$$\omega_m = \omega_t G_r \quad (10)$$

$$C_p(\lambda, \beta) = 0.23 \left(\frac{116}{\lambda_1} - 0.48\beta - 5 \right) \exp \frac{-12.5}{\lambda_1} \quad (11)$$

$$\lambda_1 = \left(\frac{1}{\frac{1}{\lambda - 0.02\beta} - \frac{0.0035}{3\beta + 1}} \right) \quad (12)$$

Table 2. Power dispersion at DC-link

Modes of operation	Action taken
Mode-1 : When No SPG & WPG	BES only will provide power to P_{DC} .
Mode-2 : When SPG & $WPG = P_{DC}$	Solar PV and wind will supply power P_{DC}
Mode-3: When SPG & $WPG < P_{DC}$	The difference sum of the power will be provided by Battery till it reaches $SOCB_{min}$
Mode-4 : When SPG & $WPG > P_{DC}$	Excessive solar power is used to charge the Battery system till it reaches $SOCB_{max}$

3. Design of Parameters

The main role of shunt active power filter is to inject the required amount of current at the PCC to provide distortion free supply current. The required amount of injected current is given by the control circuit by Eq. 13.

$$i_s = i_l - i_{sh} \quad (13)$$

$$V_s = V_m \sin \omega t \quad (14)$$

$$i_l = \sum_{n=1}^{\infty} i_n \sin(n\omega t + \phi_n) \quad (15)$$

$$= i_1 \sin(\omega t + \phi_1) + \sum_{n=1}^{\infty} i_n \sin(n\omega t + \phi_n) \quad (16)$$

$$P_l = V_s * i_l$$

3.1. DC Link Capacitor

The value of C_{dc} can be calculated by Eq. (17).

$$C_{dc} = \frac{\pi * i_{sh}}{\sqrt{3}\omega V_{pp}} \quad (17)$$

The V_{dc}^{ref} is selected within the allowable ratings of the proposed system. The selection of C_{dc} depends on peak to peak voltage ripple (V_{pp}) and shunt compensating current.

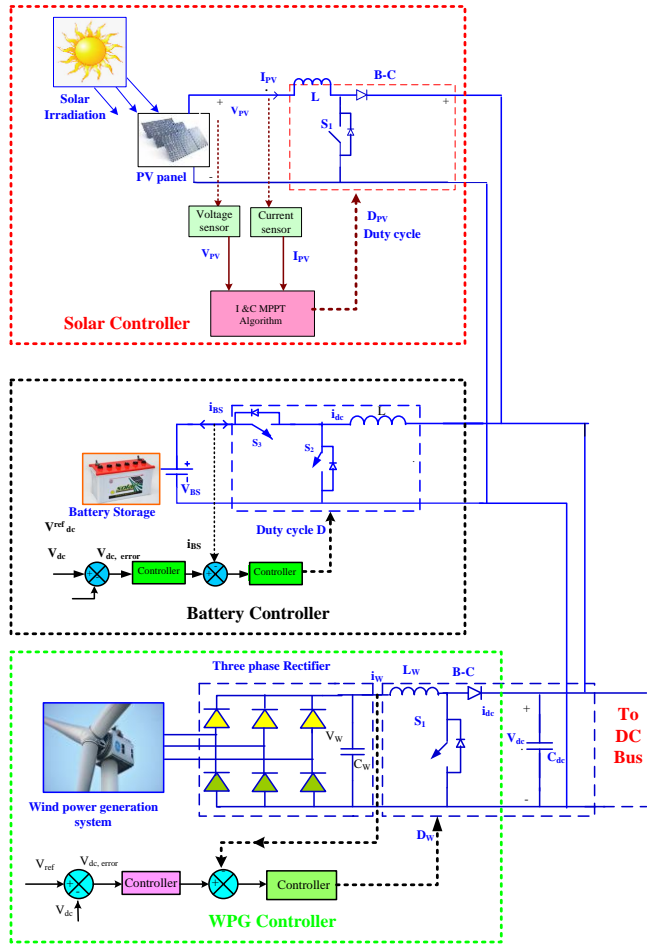


Fig. 4. Control system for external supply sources.

3.2. Inductor of Shunt VSC

The shunt VSC is linked to the network through an inductor (L_{sh}), relies on the switching frequency, ripple current and dc-link voltage as:

$$L_{sh,min} = \frac{\sqrt{3} m V_{dc}}{12 a_f f_{sh} I_{pp}} \tag{18}$$

Assuming the modulation depth (m) as 1, over loading factor (a_f) is 1.5, and switching frequency (f_{sh}) is 10 kHz, the value of L_{sh} depends on peak to peak ripples (I_{pp}).

4. STF Control

Due to the dynamic behavior of load on distribution network and sudden origin of faults leads to change in the DLCV. Therefore it is quite essential to make that voltage constant within a short duration of time without overshoot. In general, conventional control system consists of STAPF and a PLL. Where, the requirement of PLL is to isolate the positive sequence from the source voltage but in this suggested technique STF based UVGT is adopted to produce PSY from the distorted supply voltage along with acting the job of HPF, and LPF for dividing both the FC and HC of current. Thus the method suggested in this work consists of a only STF, STAPF.

As the $abc-\alpha\beta0-dq0$ transformations, design STF-UVGM are available in [25] the design part of STF, proposed ANNC was discussed in detail below:

4.1. STF

The Hong-sock developed the integral of SRFT by Eq. (19).

$$V_{xy}(t) = e^{j\omega t} \int e^{-j\omega t} U_{xy}(t) dt \tag{19}$$

Where, U_{xy} and V_{xy} are the SRF input and outputs. The transfer function $H(s)$ is obtained by adopting Laplace transform of Eq.20.

$$H(s) = \frac{V_{xy}(s)}{U_{xy}(s)} = \frac{s + j\omega}{s^2 + \omega^2} \tag{20}$$

The constant k is created to get STF. Thus, $H(s)$ is in Eq.21

$$H(s) = \frac{V_{xy}(s)}{U_{xy}(s)} = \frac{k(s + k) + j\omega_n}{(s + k)^2 + \omega_n^2} \tag{21}$$

By interchanging $U_{xy}(s)$ by $x_{\alpha\beta}(s)$ and $V_{xy}(s)$ by $x'_{\alpha\beta}(s)$, Eq. (22)-(23) is received:

$$x'_{\alpha} = \left(\frac{k}{s}\right) [x_{\alpha}(s) - x'_{\alpha}(s)] - \frac{\omega_n}{s} .x'_{\beta}(s) \tag{22}$$

$$x'_{\beta} = \left(\frac{k}{s}\right) [x_{\beta}(s) - x'_{\beta}(s)] - \frac{\omega_n}{s} .x'_{\alpha}(s) \tag{23}$$

The accuracy of getting results is inversely proportional to the k constant. The STF control technique is shown if Fig. 5.

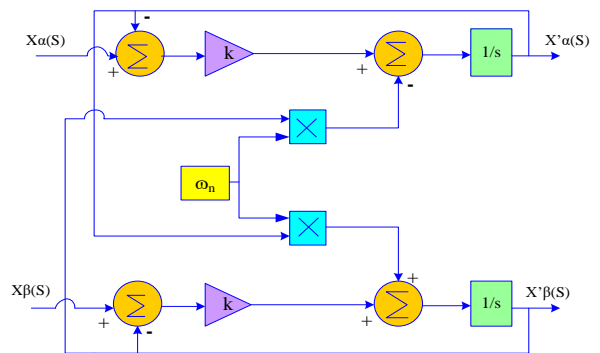


Fig. 5. STF.

4.2. Shunt VSC

The key role of STAPF is to reduce distortions in the current signal thereby reducing THD by supplying appropriate compensating current while regulating DLCV. ANFIS is

implemented for minimizing the THD and regulating the stable DLCV in a short duration during dynamic load variations. The controller of proposed method is given in Fig. 6.

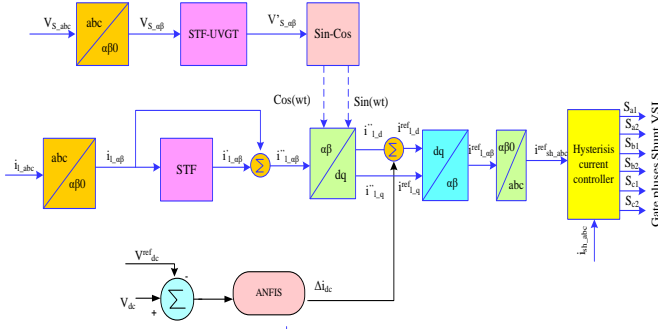


Fig. 6. ANFIS for Shunt Converter.

4.2.1. Proposed ANFIS for DC link balancing

The ANFIS is suggested to maintain constant DLCV. The suggested ANFIS is an intelligent hybrid controller with the combination of ANN and Fuzzy logic features. However, for maintaining DLCV constant, the chosen reference DLCV is compared with respect to the obtained DLCV; and its output Error (E), change in Error (CE) is considered as inputs. The inputs fed to the ANNC are initially trained according to the triangular MSF to produce the best as shown in Figure 7. ANFIS mainly consists of five layers, the 1st layer (Fuzzification) the outputs of this layer are fuzzy MSF given by Eq. 24 shown in Fig. 7

$$\begin{aligned} \mu_{A_i}(x), i = 1,2, \\ \mu_{B_j}(y), j = 1,2. \end{aligned} \tag{24}$$

Where, $\mu_{A_i} \mu_{B_j}$ are the MSF outputs obtained from the 1st layer.

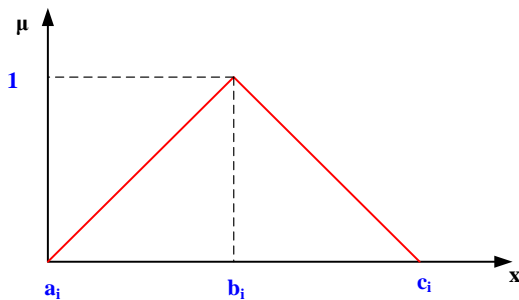


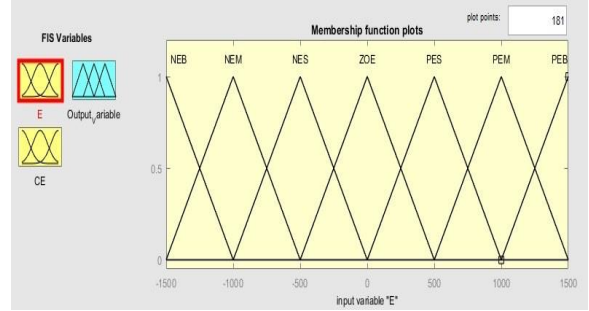
Fig. 7. Triangular MSF.

The mathematical representation of triangular MSF is given by Eq. 25.

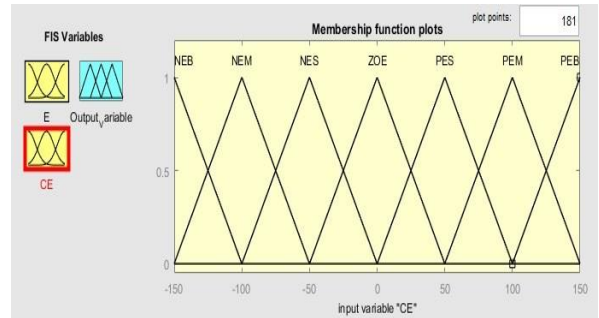
$$\mu_{A_i}(x) = \max(\min(\frac{x - a_i}{b_i - a_i}, \frac{c_i - x}{c_i - b_i}), 0) \tag{25}$$

Where, the range (universe of discourse) of x is $x_{max} - x_{min}$ (upper and lower bonds) and b_i is the point of maximum support of the fuzzy set i. The Negative-Big (NEB), Negative medium (NEM), Zero (ZOE), Positive small (PES), Positive

Big (PEB), Positive medium (PEM) and Negative-Small (NES) are considered as input/ outputs. The inputs and outputs of MF are shown in Fig 8. Table 3 exhibits the fuzzy-rule-base.



(a) MF for E



(b) MF for CE

Fig. 8. Fuzzy MF for E, CE.

However, in the 2nd layer (weighting of fuzzy rules) the AND operator is applied, and calculates the firing strength w_i by adopting MSF computed in 1st layer whose output is calculated by Eq. (26).

$$w_k = \mu_{A_i}(x) * \mu_{B_j}(y), i, j = 1,2. \tag{26}$$

E	CE						
	PEB	PEM	PES	ZOE	NES	NEM	NEB
NEB	ZOE	NES	NEM	NEB	NEB	NEB	NEB
NEM	PES	ZOE	NES	NEM	NEB	NEB	NEB
NES	PEM	PES	ZOE	NES	NEM	NEB	NEB
ZOE	PEB	PEM	PES	ZOE	NES	NM	NEB
PES	PEB	PEB	PEM	PES	ZOE	NES	NEM
PEM	PEB	PEB	PEB	PEM	PES	ZOE	NES
PEB	PEB	PEB	PEB	PEB	PEM	PES	ZOE

The normalization of values takes places in the 3rd layer received from the previous layer. Each node reaches normalization by evaluating the ratio of the kth rule's firing strength (truth values) to the summation of all rule's firing strength is given Eq. (27).

$$\bar{w}_k = \frac{w_k}{w_1 + w_2} \quad k = 1,2. \tag{27}$$

The self-adaptive ability of the ANNC is carried out by applying the inference parameters (p_k, q_k, r_k) in the 4th layer (defuzzification) output is given by Eq. (28).

$$\overline{w_i f_i} = \overline{w_i} (p_k u + q_k v + r_k) \tag{28}$$

Lastly, at the 5th layer inputs are get added up to produce the desired total ANFIS output by Eq. (29).

$$f = \sum_i \overline{w_i f_i} \tag{29}$$

Fig. 9 shows the internal structure of the ANFIS. The ANFIS is trained to maintain constant DLCV and to generate reference current signals. However, for maintaining the DLCV constant, reference DLCV (V^{ref}_{dc}) is compared with the actual DLCV (V_{dc}); and its error is chosen as input data, Δi_{dc} .

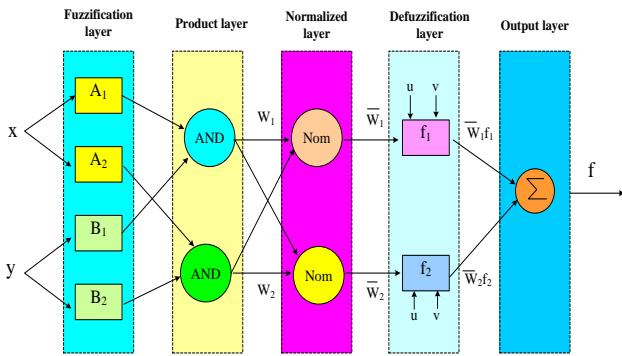


Fig. 9. Structure of ANFIS.

5. Simulation and Results

The 3 ϕ distribution system was selected to observe the performance of the proposed ANFIS. The system was developed in Matlab version 2016 given in Figure 10. Five different test cases with several arrangement of non-linear balanced and unbalanced loads, variable irradiation with constant 25^oc temperature were chosen to analyze the working of ANFIS as listed in Table-5. However, the THD were evaluated for all test cases in addition to the comparison with PI-C, SM-C, ANNC methods along with controllers that are present in the survey as listed in Table 6. The selected shunt and load ratings in this work are given in Table 4.

Table 4. Shunt converter ratings with loads considered

Supply	$L_s = 1e-3$ H, $V_s = 380$ V ; $f = 50$ Hz
SUAPF	$C_{sh} = 6E-6$ F; $L_{sh} = 1e-3$ H
DCLink	$C_{dc} : 2200$ microfarad ; $V^{ref}_{dc} = 700$ Volts

Here, in case-1 as given in table 5 to exhibit the performance of STAPF balanced Load 2 & 4 is chosen. The developed technique decreases the distortions in current signal as shown in Fig 11(a) which is reflected in the THD. Initially the grid is supplied till 0.2 sec with Load 1 after that island microgrid supplies to the load. The supply current signal THD is diminished to 4.17%, which is seems to be lower as listed

in Table 6 when compared to state of art literature and controller executed. Additionally, the controller regulates a stable DLCV at 1000W/m2 irradiation, 11m/sec with a constant temperature of 25^oc as exhibited in Figure 11 (b).

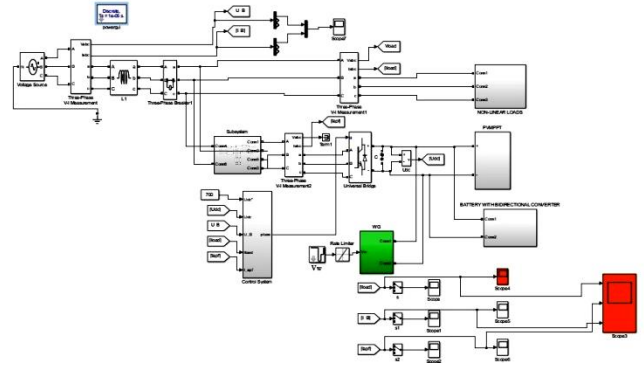


Fig. 10. Shunt filter model with loads in Simulink.

In case2, the balanced load 1 is connected till 0.2 sec with grid operation later load 3 is connected under islanded micro-grid with variable irradiation and 11m/sec wind velocity. The proposed ANFIS suppresses the THD effectively to 2.94% as shown in Fig. 12(a) and maintains DLCV constant during irradiation and load variation as seen in Figure 12 (b). However, the proposed system reduces harmonics in the load current but not distortions as the grid supply is zero.

In case3, similar to case1 & 2 load 1 is connected till 0.2 sec. After 0.2sec load 3 & 4 were connected. The proposed ANFIS reduces harmonics which inturn reflects THD to 3.01% which is lower than IEEE standards as given in Fig 13(a). It also balances DLCV constant during 1000w/m2 irradiation and variable wind velocity as shown Fig. 13(b). In case4, load 2 and 4 were chosen with a variable irradiation and wind velocity. The ANFIS suppress the distortions in the current signal and minimizes the THD to 4.57% as shown in Fig 14 (a). However, Fig.14 (b) shows that suggested ANFIS performs successfully at load, solar irradiation and wind velocity simultaneously. In addition, the THD frequency spectrum for all the cases is as shown in Fig.15.

Table 5. Test cases

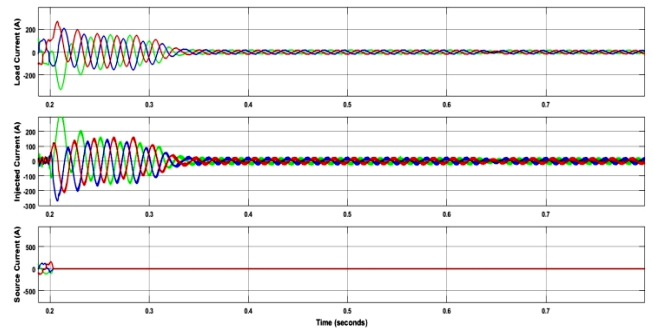
Condition / Load	Case1	Case2	Case3	Case4
Load 1: Rectifier load R=5, L= 30mH	✓	✓	✓	✓
Load 2 : P= 20e3 watts, Q= 100vars	✓		✓	✓
Load 3 : R= 15, L= 5mH; R= 10, L= 30mH; R= 5, L= 15mH			✓	
Load 4: Induction motor LC = 400 mH, 50 μ F, R = 500 Ω	✓	✓	✓	✓

Table 5. continued

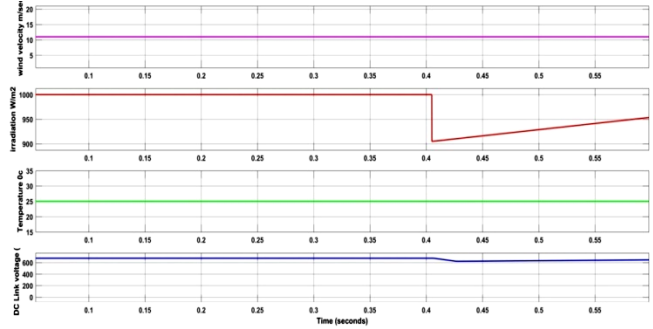
Condition / Load	Case1	Case2	Case3	Case4
Constant irradiation (G) of 1000W/m2	✓		✓	✓
Variable irradiation		✓		✓
Constant wind velocity of 11m/sec	✓	✓		
Variable wind velocity			✓	✓
Current	✓	✓	✓	✓
THD	✓	✓	✓	✓

Table 6. % THD comparison

Method	Case1	Case2	Case3	Case4
PIC	5.82	7.68	5.25	6.01
SMC	4.55	4.74	4.23	5.01
ANNC	4.29	3.45	3.05	4.70
[PI -Fuzzy]	3.07	---	---	---
[PI]	2.28	---	---	---
[FLC]	2.96	---	---	---
ANFIS	4.17	2.94	3.01	4.57

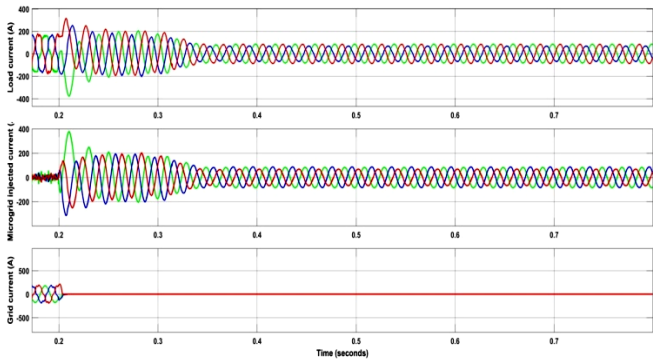


(a) i_l, i_{sh}, i_s

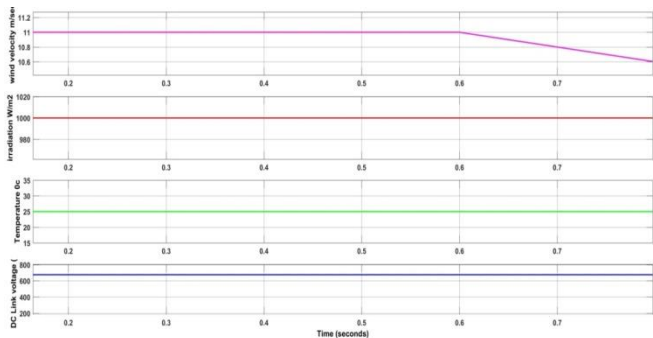


(b) irradiation, T, DLCV

Fig. 12. Proposed system for case-2.

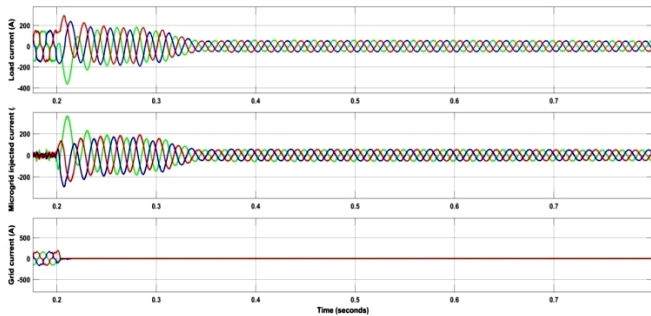


(a) i_l, i_{sh}, i_s

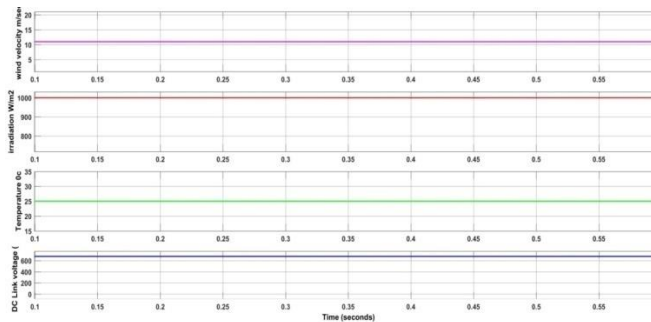


(b) irradiation, T, DLCV

Fig. 13. Proposed system for case-3.



(a) i_l, i_{sh}, i_s



(b) Irradiation, T, DLCV

Fig. 11. Proposed system for case-1.

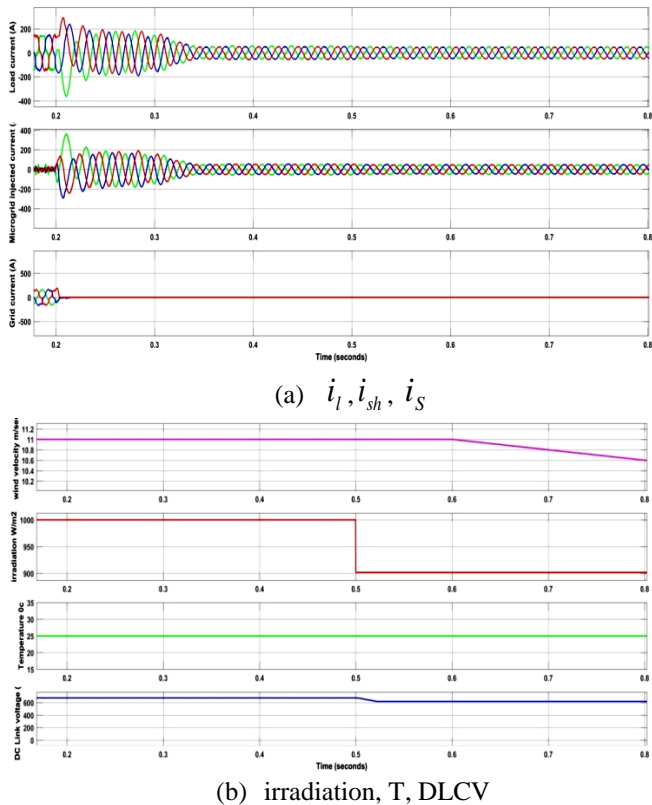


Fig. 14. Proposed system for case-4.

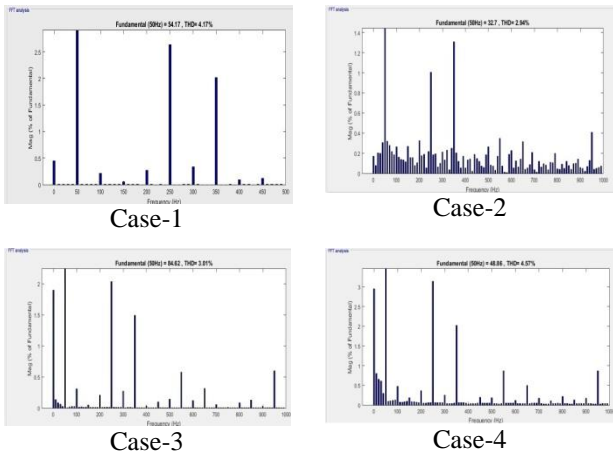


Fig. 15. THD spectrum.

6. Conclusion

The ANFIS is designed for Solar, wind and BES (microgrid) integrated shunt VSC with an objective of regulating DLCV and reducing THD and to observe the performance of the system under constant solar temperature 25°C during variable load, solar irradiation, and wind velocity. The STF is developed to eliminate the necessity of PLL. From the observation of the performance of developed technique on four different combinations of test studies it clearly exhibits that it diminishes the load current THDs. Moreover, by the comparative investigation with PI-C, SM-C and ANNC it is has been proved that the performance of developed method was much better than other controllers. The work in future can

be expanded to obtain better results with metaheuristic algorithms with multilevel converters.

References

- [1] G. Vijayakumar, N. Gupta and R. A. Gupta, “Mitigation of power quality problems using shunt active power filters: A comprehensive review”, 12th IEEE Conference on Industrial Electronics and Applications (ICIEA), 18-20 June 2017.
- [2] M. Kesler, and E. Ozdemir, “Synchronous-reference-frame-based control method for UPQC under unbalanced and distorted load conditions”, IEEE Transactions on Industrial Electronics, Vol. 58, No. 9, pp. 3967-3975, September 2011.
- [3] M. Suresh, and A. K Panda, “PI and Fuzzy Logic Controller based 3-phase 4-wire Shunt active filter for mitigation of current harmonics with Id-Iq control strategy”, Journal of Power Electronics, Vol. 11, No. 6, pp. 914-921, Nov 2011.
- [4] S R. Das, P. K. Ray, A. Mohanty and G. Panda, “Power quality enhancement in PV and battery storage based microgrid using hybrid active filter”, 2020 3rd International Conference on Energy, Power and Environment: Towards Clean Energy Technologies, 5-7 March 2021.
- [5] M. Suresh and A. K. Panda, “RTDS hardware implementation and simulation of SHAF for mitigation of harmonics using p-q control strategy with PI and Fuzzy logic controllers”, Frontiers of Electrical and Electronic Engineering, Vol. 7, No. 4, pp. 427-437, Jun. 2012.
- [6] C.L. Hsiung, “Intelligent neural network-based fast power system harmonic detection”, IEEE Transactions on Industrial Electronics, Vol. 54, No. 1, pp. 43-52, Feb.2007.
- [7] P.K.Dash, S.K.Panda, T.H.Lee J.X.Xu and A.Rou tray, “Fuzzy and neural controllers for dynamic systems: an overview”, IEEE, May 1997.
- [8] S. Devassy, and B. Singh, “Design and performance analysis of three-phase solar PV integrated UPQC”, ICPS, IEEE-March 2016.
- [9] V. K Krishna, S. K. Dash and K.R Geshma, “Development and analysis of power quality by using fuel cell based shunt active power filter”, 2020 2nd International Conference on Innovative Mechanisms for Industry Applications (ICIMIA), 5-7 March 2020.
- [10] S. Koganti, K.K. Jyothi and S. Salkuti, “Design of multi-objective-based artificial intelligence controller for wind/battery-connected shunt active power filter”, Algorithms, Vol. 15, No. 8, pp. 256, 2022, July-2022.
- [11] K. Chandrasekaran, J. Selvaraj, C. R. Amaladoss and L. Veerapan, “Hybrid renewable energy based smart grid system for reactive power management and voltage profile enhancement using artificial neural network”, Energy Sources, Part A: Recovery, Utilization, and

- Environmental Effects, Vol. 43, No. 19, pp. 2419–2442, March 2021.
- [12] A. Ramadevi, K. Srilakshmi, P. Balachandran, Ilhami Colak , C. Dhanamjayulu , and Baseem Khan, “Optimal design and performance investigation of artificial neural network controller for solar- and battery-connected unified power quality conditioner”, International Journal of Energy Research, Vol. 2023, PP. 3355124, April-2023.
- [13] Krishna Sarker, Debashis Chatterjee and S. K. Goswami, “A modified PV-wind-PEMFCs-based hybrid UPQC system with combined DVR/STATCOM operation by harmonic compensation”, International Journal of Modeling and Simulation, Vol.41, No.4, pp. 243-255, March 2020.
- [14] T. S. Saggi, L. Singh, B. Gill and O. P. Malik, “Effectiveness of UPQC in mitigating harmonics generated by an induction furnace”, Electrical power components and systems, Taylor & Francis, Vol. 46, No. 6, pp. 629-636, Nov-2018.
- [15] S.S. Dheeban and N.B. Muthu Selvan, “ANFIS-based power quality improvement by photovoltaic integrated UPQC at distribution system”, IETE Journal of Research, Feb-2021.
- [16] Mahmoud Ebadian, Mohammad Talebi and Reza Ghanizadeh, “A new approach based on instantaneous power theory for improving the performance of UPQC under unbalanced and distortional load conditions”, *Automatika, Journal for Control, Measurement, Electronics, Computing and Communications*, DOI: 10.7305/automatika.2015.07.750, Vol. 56, No. 2, pp. 226-237, Jan-2017.
- [17] M. Abdusalama, P. Poure, S. Karimia and S. Saadate, “New digital reference current generation for shunt active power filter under distorted voltage conditions”, Vol. 79, pp. 759–765, Dec-2009.
- [18] S. Samal and P. K. Hota, “Design and analysis of solar PV-fuel cell and wind energy based microgrid system for power quality improvement”, *Cogent Engineering*, 2017, 4, 1-22.
- [19] V. Vinothkumar, and R. Kanimozhi, “Power flow control and power quality analysis in power distribution system using UPQC based cascaded multi-level inverter with predictive phase dispersion modulation method”, *Journal of Ambient Intelligence and Humanized Computing* 2021, 12, 6445–6463.
- [20] K. Srilakshmi, K. K. Jyothi, G. Kalyani & Y. S.P Goud. “Design of UPQC with solar PV and battery storage systems for power quality improvement”, *Cybernetics and Systems: An International Journal*, March-2023.
- [21] V. Veera Nagireddy, V. R. Kota, D. V. Ashok Kumar, “Hybrid fuzzy back-propagation control scheme for multilevel unified power quality conditioner”, *Ain Shams Engineering Journal*, 9(4). 2709-2724. (2014). <https://doi.org/10.1016/j.asej.2017.09.004>
- [22] K. Srilakshmi, C. N. Sujatha, P. K. Balachandran, L. Mihet-Popa, and N. U. Kumar, “Optimal Design of an Artificial Intelligence Controller for Solar-Battery Integrated UPQC in Three Phase Distribution Networks”, *Sustainability*, Vol. 14, No. 21, Oct-2022.
- [23] K. Srilakshmi , N. Srinivas , P. K. Balachandran , J.G.P. Reddy, S. Gaddameedhi, N. Valluri, S. Selvarajan, “Design of soccer league optimization based hybrid controller for solar-battery integrated UPQC”, *IEEE Access*, Vol. 10, pp. 107116-107136, Oct-2022.
- [24] F. Ayadi, I. Colak, I. Garip, H. Bulbul, “Impacts of Renewable Energy Resources in Smart Grid”, 8th International Conference on Smart Grid, Paris, pp. 183-188, June 2020.
- [25] I. Colak, R. Bayindir, S. Sagioglu, “The effects of the smart grid system on the national grids”, 8th International Conference on Smart Grid, Paris, pp. 122-126, June 2020.
- [26] S. Jaber, A. M. Shakir, “Design and simulation of a boost-microinverter for optimized photovoltaic system performance”, *International Journal of Smart Grid*, Vol. 5, No. 2, pp. 1-9, June 2021.
- [27] S. S. Dash, “Tutorial 1: Opportunities and challenges of integrating renewable energy sources in smart” 6th International Conference on Renewable Energy Research and Applications, San Diego, CA, USA, 5-8 Nov. 2017.
- [28] M. Tsai, C. Chu, W. Chen, “Implementation of a serial ac/dc converter with modular control technology”, 7th International Conference on Renewable Energy Research and Applications, Paris, France, pp. 245-250, Oct. 2018.
- [29] A. Belkaid, I. Colak, K. Kayisli, R. Bayindir, “Improving PV system performance using high efficiency fuzzy logic control”, 8th International Conference on Smart Grid, Paris, pp.152-156, June 2020.